Sizing of essential SHM components of IVHM architecture and computing the relevant costs via scalable simulation

H. Meyer[1], T. Odinets[2] and V. Gollnick[3]

[1] Research Assistant German Aerospace Center Institute of Maintenance, Repair and Overhaul
[2] Master Student at Technical University Hamburg
[3] Professor Air Transport Systems Technical University Hamburg

Abstract

Application of Integrated Vehicle Health Management (IVHM) tools to aircraft repair and maintenance use cases can reduce maintenance periodicity, durance and costs, delays and turnaround time while optimizing planned vehicle maintenance and logistics. Whereas, structural health monitoring as a part of IVHM is focused on developing the technical means for performing automated inspections of aircraft structures. In prospect, successful implementation of Structure Health Monitoring (SHM) techniques can allow a lighter weight design for structure in future aircraft. Inside of the CleanSky II project DEMETER the benefits of changed design rules are evaluated. The main purpose of this paper is to show a tool for performing the sizing of essential SHM components and computing the relevant costs. This allows an evaluation of SHM monitored structures with the cost-benefits included.

Therefore a generic aircraft model is developed, to calculate the design relevant parameter from a small set of public available parameter. Several types of sensors monitor different failure causes related to the structure are selected for simulation. Major parameters of SHM system such as weight, power consumption and generated data (see Figure 1) amount are estimated via a scalable simulation in relation to aircraft size and SHM sensors penetrability. The data amount will generate design requirements on data processing and storage. The simulation will also support decision-making related to selecting an optimal avionic architecture depending on quantity of sensors and generated data amount. The costs due to increasing of fuel consumption by weight change and power consumption after installation of sensing system are analyzed. In a show case the changed payload-range diagram of an A320 will show the impact with changed design and implemented SHM.

A/D *Analog / Digital*
AAC *Airline Administrative Control*
ACARS *Aircraft Communications Addressing and Reporting System*
ADCN *Aircraft Data and Communication Network*
AOC *Aeronautical Operational Control*
ARINC *Aeronautical Radio Incorporated*
ATC *Air Traffic Control*
AWG *American wire gauge*
CAN *Controller Area Network*
D/A *Digital / Analog*
DIMA *Distributed Integrated Modular Avionics*
EDGE *Enhanced Data Rates for GSM Evolution*
FBG *Fibre Bragg Grating*
Flight ID *Flight Identifier*
GPRS *General Packet Radio Service*
HF *High frequency*
HFDL *HF data link*
I/O *Input / Output*
ICAO *International Civil Aviation Organization*
IMA *Integrated modular avionics*
IVHM *Integrated Vehicle Health Management*
LAN *Local Area Network*
MSN *Message Sequence Number*
MTOW *maximum take off weight*
OEW *Operating Empty Weight*
PHM *Prognostics and Health Management*
RGS *remote ground stations*
SATCOM *Satellite Communications*
SFC specific fuel consumption
SHM *Structure Health Monitoring*
UMTS *universal mobile telecommunication system*
VDL *VHF data link*
VHF *Very high frequency*

1 Introduction

In [1], a study on the potentials of Prognostics and Health Management (PHM) is carried out. According to [1], weight saving can be achieved through a new design approach wherein Factors of Safety for structures are reduced. A justification for reduction of Factors of Safety is originated from the fact that continuous structural health monitoring can be performed and, thus, the damage tolerance criteria can be reduced since damage is discovered and repaired before it gets critical. The estimation of influence of Factor of Safety reduction on selected parameters is performed for Airbus A320-200. In the whole, the weight savings for a decrease of the Factor of Safety of about 30 % (from 1.5 to 1) from fuselage and wing equals up to 5 % of the OEW [1]. The weight savings expectedly lead to a reduction of fuel consumption and emissions.

The weight saving potential identified by [2], associated to the integration of a structural health monitoring, is approximately 9%. This is reached by reduction of the damage size for damage tolerant structures. In order to achieve a real estimate of the net weight saving, the negative effects of an SHM system have to be considered. The goal of the tool is to calculate the negative effects for the aircraft

design, such as additional weight, power consumption and data transfer.

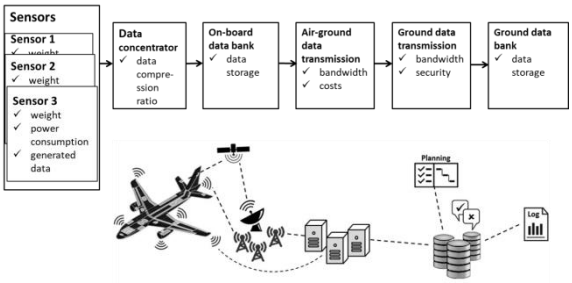

Figure 1: Simulation approach scheme

To carry out the sizing of essential SHM components of IVHM architecture and computing the relevant costs, the following challenges must be solved:

- Determination the required quantity of sensors and instruments per aircraft structure
- Reveal of alternative ways of data transfer, compression, and storage
- Performing a scalable simulation to evaluate the dependencies of parameters of sensing systems from size of aircraft and penetrability level of sensors

On one hand, the developed method should give a first estimate of the system size for new designs. On the other hand, an order of magnitude for weight and power consumption should be determined for individual structural elements of existing aircraft.

The parameters of sensing systems and requirements on data transmission and store are evaluated with the help of MATLAB. The input parameters, such aircraft, sensor, power supply cable and data transfer parameters, are collected in a general input file and can be varied, and the outputs are obtained after performing of simulation routine. Figure 2 shows the basic tool architecture.

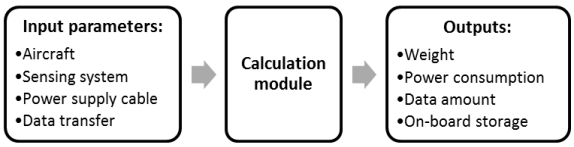

Figure 2: Simulation principle

2 Generic Aircraft

For the calculation of the required number of sensors for aircraft structures, it is necessary to define the relations between such input variables as wing span, wing area, taper ratio, length and diameter of fuselage, and other aircraft parameters. In the simulation a actual aircraft can be selected or the basic parameter can be inserted and the structure area is calculated by the tool itself.

In the simulation, aircraft structures are divided into the following groups: fuselage, wings, horizontal tail, vertical tail, and nacelle.

In the next paragraphs, exemplary the calculation of the fuselage is described. The method of the regression functions is used for all structures of the aircraft. Therefore the tool can be used to estimate the SHM components for legacy aircraft, and additional to estimate the components for new aircraft designs in the early design phase.

2.1 Fuselage modeling

The simplest way of modelling fuselage's shape is assuming it to be a cylinder. The length of cylinder is equal to the length of fuselage. Nevertheless cockpit and tail sections are smaller compared to the center section. Therefore the fuselage is split into three parts: a cockpit section, a center section and a tail section, as it is shown at the Figure 3.

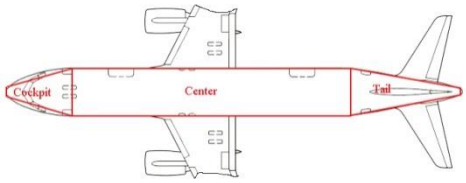

Figure 3: Fuselage modeling shape; aircraft source [3]

The lengths of cockpit and tail sections depend on fuselage diameter [4]. The parameter of cockpit and tail sections was manually measured at scaled drawings for the aircraft types mentioned in Table 1. Figure 4 shows the correlation between fuselage diameter and length of cockpit section for these types of aircraft.

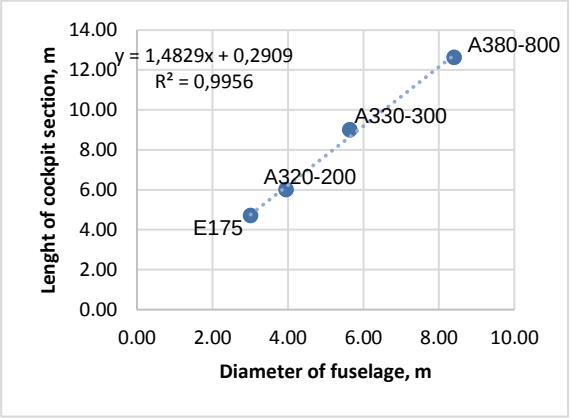

Figure 4: Cockpit section length, based on [5], [6]

The trend line formula

(1) $y = 1{,}4829x + 0{,}2909 \; R^2 = 0{,}9956$

is used for computing the length of cockpit section of a generic aircraft. The Table 1 illustrates the comparison between the actual and estimated lengths of cockpit sections.

Table 1: Comparison between the estimated and actual length of cockpit, based on [5], [6]

Aircraft	Actual	Estimated	Deviation

type	length of cockpit section, m	length cockpit section, m	
E 175	4.70	4.75	-1.16%
A320-200	6.00	6.15	-2.47%
A330-300	9.00	8.65	+3.84%
A380-800	12.62	12.76	-1.13%

The Figure 5 shows correlations of diameter of fuselage and length of tail section accordingly.

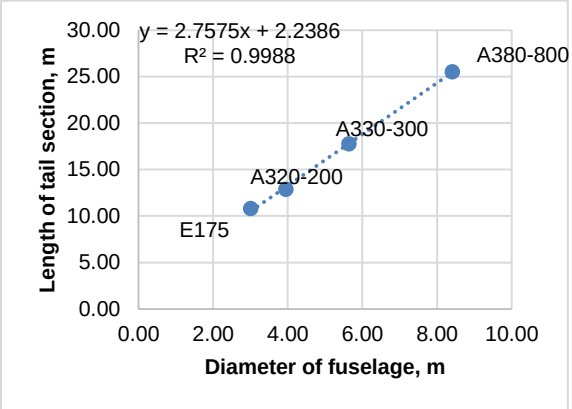

Figure 5: Tail section length, based on [5], [6]

The Table 2 illustrates the comparison between the actual and estimated lengths of tail sections. The length of a generic aircraft tail section is computed using the trend line formula:

(2) $y = 2{,}7575x + 2{,}2386 \; R^2 = 0{,}9988$

Table 2: Comparison between the estimated and actual length of tail section [5], [6]

Aircraft type	Actual length of tail section, m	Estimated length of tail section, m	Deviation
E 175	10.80	10.54	2.42%
A320-200	12.84	13.13	-2.26%
A330-300	17.75	17.79	-0.23%
A380-800	25.50	25.43	+0.28%

The center section length of the fuselage is calculated with

(3) $l_{center} = l_{fus} - l_{cockp} - l_{tail}$

where l_{fus} is fuselage length.

A surface area of fuselage can be found as a sum of areas of these three sections. It is assumed that the cockpit section has a starting diameter of 20% of the input diameter D of fuselage. The cockpit diameter linearly increases till the diameter of fuselage D. The diameter of center section is equal to the input diameter. The tail section starts with a diameter D and decreases to 20% of this diameter.

2.2 Surface area calculation

The surface area of the fuselage is calculated with the following formulas. It is assumed, that the windows and the doors are neglected for the calculation of fuselage surface area.

Surface area of cockpit:

(4) $S_{cockp} = \pi \cdot \left(\frac{0.2 \cdot D}{2}\right)^2 + \pi \cdot (0.2 \cdot \frac{D}{2} + \frac{D}{2}) \cdot l_{cockp}$

Surface area of center section:

(5) $S_{center} = \pi \cdot D \cdot l_{center}$

Surface area of tail section:

(6) $S_{tail} = \pi \cdot \left(\frac{D}{2} + 0.2 \cdot \frac{D}{2}\right) \cdot l_{tail} + \pi \cdot \left(\frac{0.2 \cdot D}{2}\right)^2$

Total surface area of fuselage:

(7) $S_{fus} = S_{cockp} + S_{center} + S_{tail}$

The windows and the doors are neglected for the calculation of fuselage surface area.

3 Sensor selection

Structural health monitoring is focused on developing the technical means for performing automated inspections of aircraft structures.

Figure 6 shows the dominant loads that establish basis for the dimensioning criteria shall be met in all parts of the aircraft structure. The typical sources for the loads are: internal pressure, aircraft weight, aerodynamic loads and maneuver loads. Sources of these loads vary during the different flight phases. [7]

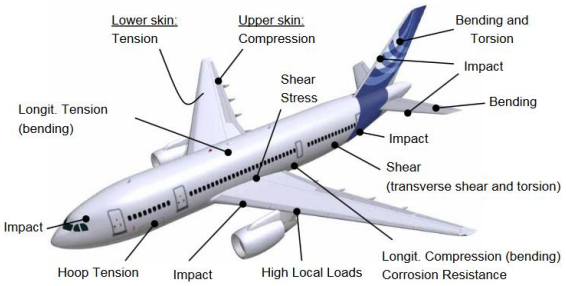

Figure 6: Dominating loads [7]

A large number of various types of sensors are needed to provide real-time information of aircraft structures health condition. The sensors measure a multitude of parameters including pressure, vibration, load, strain and enable to identify damage and estimate the location. The environmental conditions have to be monitored for providing warnings in the case of corrosive conditions [8].

Sensing systems for health monitoring consist of some or all of the following components: transducers for converting the measured variable

(temperature, strain) in an electrical signal; actuators that apply a prescribed input to the system; A/D and D/A converters; power supply source; telemetry; software for data processing (algorithms, feature extraction procedures, etc.) and memory for data storage [9].

The number of sensors depends on the covered area and the range of the specified sensor. Nevertheless, the decision regarding the number and location of sensors must balance the economic aspect of the sensing system with the system reliability. Traditional sensing approach utilizes few sensors distributed in a certain sequence on the structure. A main problem of this approach is that, in the case of fail of one sensor, the system cannot provide reliable information about structure damages anymore. Sensors are usually placed near expected damage locations. There are studies that have developed genetic algorithms or neural networks to optimize a given sensor budget [9].

The aircraft structure was split into the areas based on schemes shown in Figure 6 and Figure 7. There is no single monitoring technology for detecting all types of damages or structural degradation. The specific load cases can be monitored by suitable structural health monitoring techniques [10]. The assumptions for shape modeling of aircraft structures are also illustrated.

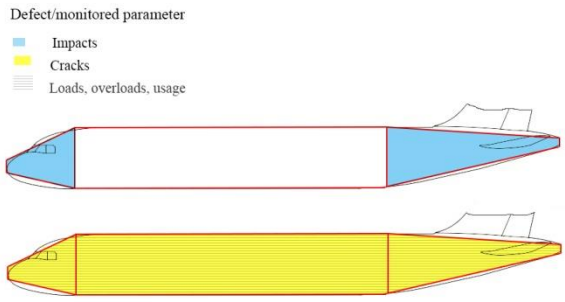

Figure 7: Defects/monitoring parameters at fuselage; aircraft source [3]

As it can be seen at the Figure 7, impact effects have to be monitored at the cockpit and tail sections. The loads, overloads, usage and crack monitoring must be provided at the whole fuselage area.

For the aircraft group monitoring, it is assumed that the aircraft surface is split into generic panels with dimensions 1×1m. Health monitoring sensors can be installed on or embedded within the structure and perform the tasks analogous to earlier manual inspection actions. The number of sensors per generic panel can be adjusted in the tool for the different dominating loads.

It is assumed that structure sensors are applied to all primary structures like the main wing, fuselage and empennage. The total number of sensors and required instruments result from the total number of generic panels needed to cover the aircraft surface.

The data amount produced by sensors depends on sampling frequency. In general, the data rate can be calculated using the following equation:

(8) $C = n_{ch} \cdot B \cdot RES$

where B is sampling frequency, RES is resolution and n_{ch} is the number of channels, e.g. number of interrogator channels for FBG sensing system, number of amplifier's channels (typically one) or number of sensors.

The typical resolution is 12 Bit [11]. The systems with high sensitivity can have resolution of 24 or 32 Bit.

4 Data Bus Architectures

The following paragraphs describe the basic data bus architectures. The chosen architecture has an influence on the possible transmission rate per data bus. According to the SHM penetration, the selected architecture has a significant influence on the system weight. In the developed tool the three different architectures are calculated simultaneously, to enable a decision for the best suitable architecture.

4.1 Federated architecture

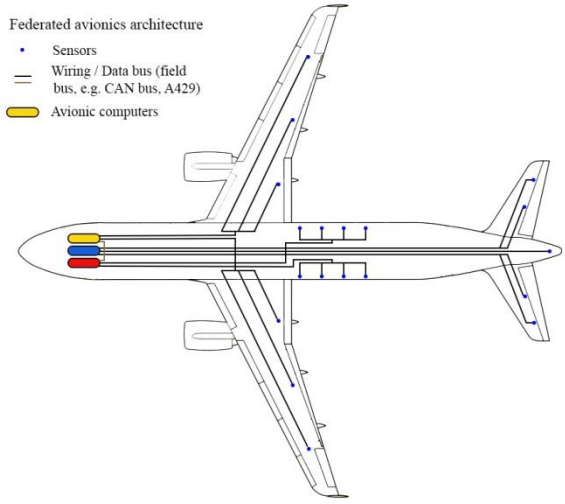

Figure 8: Federated avionics architecture based on [12] [13] [14]; aircraft source [3]

Federated avionics architecture is illustrated at the Figure 8. Each system has its own hardware performing its own functions, there is no or minor data exchange between different systems. Since a federated architecture uses dedicated task-oriented and line-replaceable computers, this architecture could be applied to the aircraft systems that were not traditionally avionics systems such as fuel systems, landing gear systems and etc. ARINC 429 is typically used for data transferring between the processing centers on the aircraft.

There are some disadvantages of this architecture type. New or added system functionality often causes major system redesign, integration test and

verification work. Implementing health management functions would require new sensors, data concentrators, and a communication system. [13] Thus, number of hardware component usually grows with increasing number of functionalities and, thus, system weight also increases. [14]

4.2 Integrated modular avionics architecture

Integrated modular avionics (IMA) architecture is represented by a general-purpose centralized computing resource comprising a set of common hardware computing modules, standardized according to ATA-42. All IMA modules are located in the avionics bays. IMA architecture is used for such aircraft as Airbus A380, Boeing 777, and Airbus A400M. IMA architecture is introduced at the Figure 9.

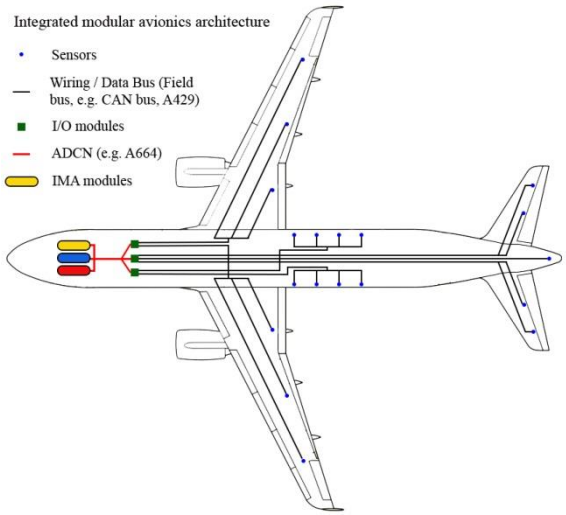

Figure 9: Integrated modular avionics architecture based on [12] [13] [14]; aircraft source [3]

Common processing includes robustly partitioned application software. Aircraft Data and Communication Network (ADCN) that is a standardized high-bandwidth data network, is used for communication. Data buses A664 and A629 perform data transfer inside of ADCN.

Periphery includes electronic and hardware components that are not parts of IMA and are connected to IMA modules or ADCN. Data transmission is often provided by CAN buses or ARINC 429. Periphery is typically represented by sensors and actuators.

Applications on the module can be reconfigured and, thus, less different types of hardware are needed. It provides up to 50% reduction of avionic components. [14]. This aspect enables significant cost reduction comparing with federated architecture. IMA architecture enables physical integration of networks, modules and I/O devices, thus, its growth and change. Process of integration and reconfiguration is rather complicated. This avionics architecture is not suitable for all aircraft systems because of data delivery delays and relative low reliability. Amount of needed cables can be also rather large. [14] [15]

4.3 Distributed integrated modular avionics architecture

Distributed Integrated Modular Avionics (DIMA) is an IMA distributed inside of the aircraft. Airbus A350 and Boeing 787 use this type of architecture. DIMA architecture (see Figure 10) provides computation close to sensors and actuators which results in reducing of cable length and amount, and, thus, faster system response. Cockpit, Cabin, Flight Control, Engines, Fuel, etc., are separated into integration areas. I/O and computational resources are partitioned. Data concentrator reduce and convert sensor data into a common digital format and then communicate this data to computer processing resources using data buses. It can also perform simple logic and alarms. DIMA requires high bandwidth communication. [15] [13]

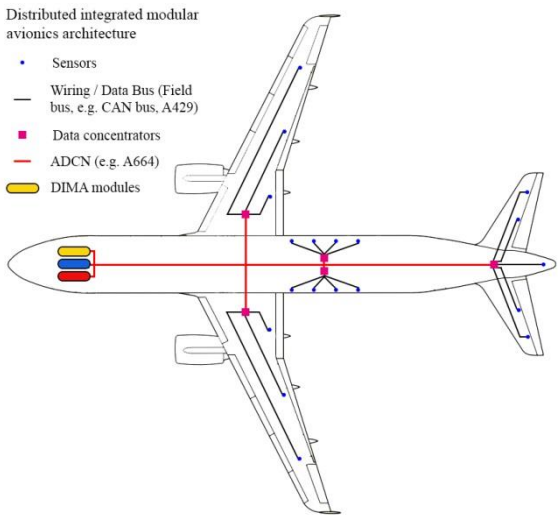

Figure 10: Distributed integrated modular avionics architecture based on [12] [13] [14]; aircraft source [3]

5 Cable weight calculation

The cable weight calculation is done in three steps. At first the number of data buses is calculated. In the next step the cable length for data buses and power supply is determined. And in the last step the wire size for the power supply is selected.

5.1 Data Bus Quantity

The quantity of cables for power supply depends on number of sensors and instruments, e.g. interrogators for FBG sensing system. To reduce the quantity of cables needed for data transfer, the analog signals can be locally converted into digital data, which are then transferred via serial data buses. Thus, the required number of data buses per

aircraft structure or component (wing, fuselage, horizontal and vertical tail, and nacelle) can be calculated this way:

(9) $n_{bus} = \frac{C \cdot n_{sensor}}{B_{bus}}$

C is the data rate of the appropriated sensor type, n_{sensor} is the quantity of instruments, e.g. interrogators or sensors per structure or component, B_{bus} is the usable bandwidth of chosen type of avionic data bus.

5.2 Wire Length

The length of cables for electrical power supply of SHM network and data transfer depends on geometrical parameters of aircraft. For the calculation of the length of cables it is assumed, that the average wire length will go to the centroid of the different structural parts.

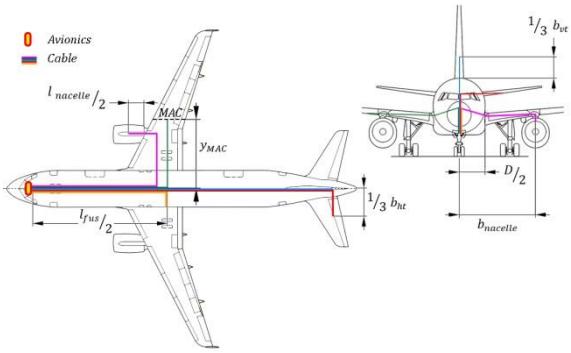

Figure 11: Cable distribution; aircraft source [3]

The length of cable for fuselage (orange lines):

(10) $l_{cable,fus} = \left(\frac{l_{fus}}{2} + \frac{D}{2}\right) \cdot k_{cable}$

Where $k_{cable} = 1.2$ is a coefficient to reflect the non-direct wire routing. The wire lengths for the other areas of the aircraft are calculated accordingly.

It is assumed that for aircraft built of metal materials, the power supply cable requires one conductor, and for aircraft built of composite materials, the power supply cable requires two conductors what means that the computed cable length must be multiplied by two.

5.3 Wire size selection

A standard known as the American wire gauge (AWG) is used for wire manufactory. [16] describes factors to be considered in selecting the size of wire for transmitting and distributing electric power. A conductor chart for continuous flow [16] that can be found in the attachment can be used to select the proper size of conductor.

In general, the wire size must be sufficient to prevent overheating of the cable and voltage drop while carrying the required current. According to [16], wires of size 26 and 24 must not be used as single wire, thus, the smallest size that can be used for simulation is 22. The power supply requirements for various types of sensors given in attachment show that the FBG interrogator has the largest power consumption, with 30 W at 12 V. All other sensors (often connected with signal conditioner or amplifier) require significantly lower electricity demand. The circuit voltage value from conductor chart is chosen 28 VDC as suitable for all sensor types. Thus, the acceptable wire size 18 can be chosen (10.40 kg/km maximum weight) for powering each FBG interrogator. It is assumed that all other selected for simulation sensors are parallel-connected and since all sensors of same sensor type require the same current value, the resulting power equals multiplication of power needed for singular sensor and number of these sensors: $P = U \cdot I \cdot n_{sensors}$. For the calculation for number of cable, a wire size 20 (6.50 kg/km maximum weight) is chosen as the smallest suitable solution, wire AWG 22 would not satisfy requirements of cable length. The number of sensor that can be powered by a singular wire can be selected which satisfy power requirements of appropriated sensors type (provided in the specification) at 28 VDC. Thus, maximum 50 piezoelectric strain sensors for impact monitoring can be powered by each wire, up to 33 piezoelectric sensors and 50 eddy current sensors for cracks monitoring accordingly. The weight of cables that realize this parallel connection of sensors is neglected.

The weight of cables for power supply and data transfer can be calculated using the following formula:

(11) $w_{cable} = l_{cable} \cdot w_{spez,cable}$

Where l_{cable} is the length and $w_{spez,cable}$ is the weight of cable

6 Data Transfer

This chapter introduces the data communication between aircraft and ground. Data can be transmitted directly during the flight through data link system or downloaded after landing. Based on the selected data transfer technology different costs occur for the operator. In the tool the different technologies are analyzed, to enable on one side the selection of the best suitable technology. On the other side a size estimation of the on-board storage can be performed. Also the different technologies are compared about the cost which will occur for data transfer.

6.1 Air-ground communication

Data link solution provides the ability to transmit digital messages between aircraft and ground stations via communication systems that are nowadays often based on VHF or SATCOM (see Figure 12) [17].

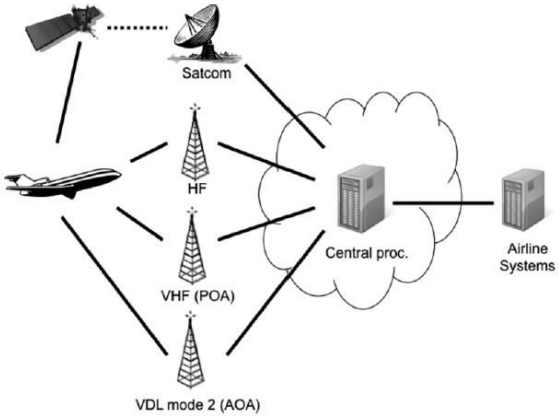

Figure 12: Air-ground communication systems [17]

Aircraft Communications Addressing and Reporting System (ACARS) is a digital datalink system for air-ground communication. The protocol was designed by ARINC in 1978. ACARS messages are transmitted using three possible data link methods: VHF or VDL (VHF data link), SATCOM and HF.

VHF ACARS is line-of-sight limited and covers only continental areas. The typical VHF range depends on altitude with a maximum of 200-mile transmission range at high altitudes. To overcome these limitations, HF data link or HFDL was added for polar region communication in 1990s. Service providers offered using geostationary communication satellites, e.g. SATCOM, to achieve the global coverage. Currently, two SATCOM systems are available: Inmarsat geostationary satellites and the Iridium low Earth orbit satellites. Civil aviation uses mainly the Inmarsat services [17] [18] [19].

Aircraft equipment consists of airborne end systems and a router. End systems are the sources of ACARS downlinks and destinations for uplinks. The downlink messages transmit information from aircraft to ground and the uplink messages transmit the information from ground stations to airplane. The router function determines which subnetwork to use, i.e., HF, VHF, or SATCOM, when routing a message from the aircraft. The service provider's ground network contains an ACARS data link service processor and a communications network that connects the processor and the remote ground stations (RGS). RGS have different configurations according to data link methods.

ACARS messages may be of three types: Air Traffic Control (ATC), Aeronautical Operational Control (AOC), and Airline Administrative Control (AAC). The flight crews request the clearances and receive them from the ground controllers through ATC messages. AOC and AAC messages are used for sending information from the aircraft to ground stations in real-time. Thus, data related to component faults and abnormal conditions can be transmitted and used for monitoring health condition of aircraft. This enables maintenance crew to plan maintenance activities and repairs when the aircraft is still in the air and optimize the maintenance process. There are various types of ACARS messages that may include fuel consumption, engine performance, aircraft position, etc. [20].

There are three major limitations in using ACARS systems for communication:

- Interfacing with ground-based Internet networks,
- Message size limitations, and
- Transmission cost [21].

Since ACARS is character-oriented instead of bit-oriented, the legacy protocols are not well-suited to support broadband applications. Data from ACARS messages have to be firstly converted into structured information to be used in modern Internet-based applications [17].

The majority of ACARS messages are typically 100 to 200 characters in length. Such ACARS messages are made of a one-block transmission from the aircraft [22]. The structure of downlink message is shown at the Figure 13.

Message head

Name	SOH	Mode	Aircraft Registration Number	TAK	Label	DBI	STX
Size	1	1	7	1	2	1	1
Example	<SOH>	2	.N123XX		5Z	2	<STX>

MSN	Flight ID	Appl Text	Suffix	BSC	BSC Suffix
4	6	0-210	1	2	1
M01A	Xx0000	Downlink	<ETX>		<DEL>

Message text | Message end & BSC

Figure 13: Downlink message [20]

One ACARS block is constrained to 220 characters within the body of the message. Every downlink transmission should include a Message Sequence Number (MSN) and Flight Identifier (Flight ID) as a part of the text message. Downlink messages longer than 220 characters will be splitted into multiple blocks (currently maximum 16), and each block will be transmitted to the ground station. The ground station collects each block until the complete message is received before processing and routing the message. The fields of ACARS messages are encoded using ISO-5 character set (A-Z, 0-9, <->, and <.>). An eighth bit is added to each character to complete the octet and render character parity odd. Maximum size limitation for ACARS downlinks is 3360 bytes and 3520 bytes for ACARS uplinks accordingly [20] [22] [19].

The range of prices for 70-80% of airlines (service provider are ARINC and SITA) is considered in **Fehler! Verweisquelle konnte nicht gefunden werden.**.

The exact values depend on specific service-level agreements between the airline and the service provider.

Table 3: Prices comparison for different data link solutions [23]

Data link	Price
SATCOM	0.2-0.6 $/kbit
VHF	0.1-0.2 $/kbit
VHF Mode 2	0.1-0.2 $/kbit
VHDL	0.2-0.3 $/kbit
Regional VHF service provider	0.3-0.5 $/kbit

Today, ACARS provides worldwide data link coverage. The ACARS air-ground VHF-subnetwork provides a data rate of 2.4kbit/s to be shared among the aircraft. VHF Mode 2 provides a data rate of 31.5kbit/s

HFDL provides data rates of 0.3, 0.6, 1.2 and 1.8kbit/s, depending on radio wave propagation conditions.

In the case of aeronautical communications, satellite communication service is regulated by ICAO. Annex 10 describes the general architecture and communication protocols. The data rates are typically amounting to tens of kbit/s.

6.2 On-ground data transmission

Transmission of stored flight performance data from aircraft parked at airport and airports is typically performed by Wi-Fi (e.g., IEEE 802.11a, b, g), wired Ethernet and cellular (e.g., GPRS, EDGE, UMTS) communication technologies. Wi-Fi connectivity is enabled through the wireless LAN and wired connectivity (Ethernet). Wi-Fi performance is highly dependent on the distance between the aircraft and airport. In [24] metrics as practical bit rate and security of possible solutions to transmit data over IP networks were summarized.

Table 4: Communication technologies and their characteristics, based on [24]

Technology	Theoretical bit rate	Practical bit rate
GSM	14.4 kbit/s	N/A
GPRS	170 kbit/s	40-50 kbit/s
EDGE	473 kbit/s	270 kbit/s
UMTS	2.0 Mbit/s	384 kbit/s
HSPDA	1.8 – 84.4 Mbit/s	1 - 6 Mbit/s
HSUPA	0.7 – 17.25 Mbit/s	1 – 1.5 Mbit/s
LTE (DL)	10 – 300 Mbit/s	N/A
LTE (UL)	5-75 Mbit/s	N/A
IEEE 802.11b	11 Mbit/s	5.8 Mbit/s
IEEE 802.11a	54 Mbit/s	24.7 Mbit/s
IEEE 802.11g	54 Mbit/s	24.7 Mbit/s

Besides, the data can be directly uploaded or downloaded into aircraft through a USB flash drive or an external hard drive [24].

In general, to transmit generated data completely within turnaround time, the required minimal transmission speed can be estimated from the following ratio:

$$(12)\ \frac{min.\ data\ trans.\ speed}{SHM\ data\ rate} \geq \frac{flight\ time}{turnaround\ time}$$

7 Fuel Consumption

Flight performance can be reflected by Breguet range equation. Based on aircraft parameters as weight, wing area and engine type, the maximum total range for given environmental conditions can be calculated. Assuming that flight velocity, lift coefficient and specific fuel consumptions are constant the Breguet formula gives a good estimation.

$$(13)\ R = \frac{L/D \cdot V}{SFC \cdot g} \cdot \ln \frac{m_{init}}{m_{final}}$$

where *R* is maximum range according to Breguet range equation, $\frac{m_{init}}{m_{final}}$ is the ratio of initial (MTOW) over final (landing) weight, *SFC* is the specific fuel consumption. According to [4], L/D ratio ranges from 18 to 22 for cruise.

Table 5: Correlation between the electrical power drain and variations in specific fuel consumption [25]

Flight phase	Thrust class	Δ SFC for 100 kW
Climb	150 kN	0.4%-0.8%
Cruise	150 kN	0.7%-1.5%
Descent	150 kN	3.0%-7.0%

The correlations from [25] can be used to translate power requirements of sensors and instruments and, thus, the electrical energy consumption of health monitoring systems into variations of specific fuel consumption (SFC). The SFC changes according to the power drain for conventional jet engine aircraft, as it is shown in **Fehler! Verweisquelle konnte nicht gefunden werden.** for 150kN thrust class engines, depending on flight phase.

It is necessary to notice that some other factors may either influence variations in SFC during different flight phases, e.g. variations of drag during different flight phases due to changes in angle of attack.

For an engine CFM56-5 used in the reference aircraft A320-200, the SFC= 16.86 (g/s)/kN [26]. Assuming a density of jet fuel around 0.8 kg/l and fuel price 139 cts/gal [27] or ~0.50 $/kg, it is possible to estimate additional costs due power consumption and weight of a SHM system.

8 Results

Numerical values presented at Figure 14 provide a briefly look on some parameters of a fictitious SHM system for the reference model Airbus A320-200. This example system is only for demonstration calculated, even if the author is clear that such full coverage system would not be implemented. A real system would focus on load paths or impact areas monitoring. The following assumptions were made for the calculations:

- Full coverage
- New structural design
- New data bus architecture (DIMA)
- 10 strain sensor per m²
- 5 impact sensor per m²
- Dominating loads as shown in Figure 6.

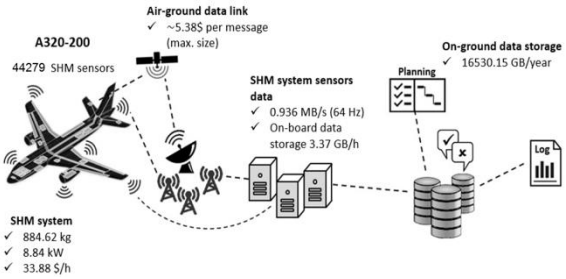

Figure 14: Results of simulated SHM system

The total number of sensors of all types for the simulated SHM system equals 44279. This introduces an additional weight of around 885kg and a power consumption of 8,84kW. This will result in a changed payload range diagram as shown in Figure 15. The reference aircraft in Figure 15 is an A320 calculated with parameter found in literature. The potential weight savings graph is calculated with the results of [1]. This includes a redesign of the aircraft and reflects therefore the maximum potential. The implemented SHM shows the reduced range due to weight and electrical power consumption. The combined graph reflects the costs and benefits of a redesigned aircraft with a SHM system included. As the range increases, compared to the reference aircraft, the system would have a beneficial effect of the operating costs.

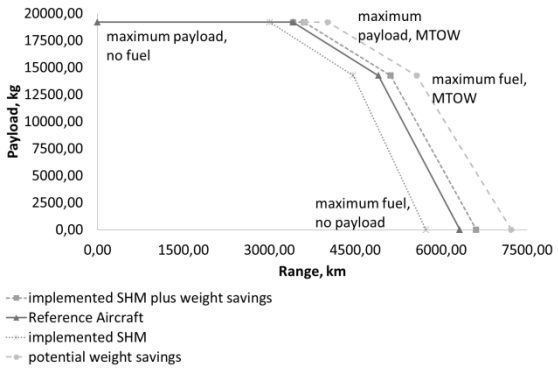

Figure 15: Payload/Range Diagram

For the use case a data amount of 3,37GB/FH is generate. As during flight only a small amount of data can be transmitted the on-board storage needs to be specified large enough to store the data between two download intervals.

Table 6: Data amount per mission

Aircraft type	Flight time	Turnaround time	Data amount per flight
Short haul	115 min	55 min	51668 Mbit

Table 6 shows the calculated data amount for a typical A320 mission. If no data reduction methods are on-board performed, the whole data must be transferred to the ground. Table 7shows the number of missions which can be transferred for different data transfer rates. If every turnaround the data are transferred a minimum of 20Mbit/s are necessary. If several missions need to be transmitted higher transfer rates are needed. The number of downloads impacts also the on-board storage size.

Table 7: Data transfer rates

Data Transfer Rate (Mbit/s)	5	20	50	100
Data Transfer per Turnaround (Gbit)	16	66	165	330
Nbr. of Missions which can be transmitted (FC)	0	1	3	6

9 Conclusion

The tool developed makes it possible to calculate a structural area of a new aircraft with a small amount of parameters. However, it is also possible to specify structural surfaces of existing aircraft. Subsequently, a number of sensors is calculated for the area according to the dominating damage types. Based on this, the extra weight (for data buses, power supply and sensors) and power consumption can be determined. It also offers the flexibility to calculate the impact for individual structural elements as done in [2]. The tool enables a first estimation of negative system influences for future SHM systems.

Acknowledgement

This study was performed within the EU-CleanSky II Project DEMETER (Grant Agreement no. 685704)

References

[1] S. Torhorst, Identification and evaluation of the potentials of Prognostics and Health Management in future civil aircraft, München: Lehrstuhl für Luftfahrtsystem TU München, 2014.

[2] C. P. Dienel, H. Meyer, M. Werwer und C. Willberg, „Estimation of airframe weight reduction due to integration of PZT based

structural health monitoring," 2018.

[3] AIRBUS S.A.S., „Airbus," 01 May 2015. [Online]. Available: http://www.airbus.com/fileadmin/media_gallery/files/tech_data/AC/Airbus-AC_A320_01_May_2015.pdf. [Zugriff am 19 December 2016].

[4] V. Gollnick, Lecture "Methoden des Flugzeugentwurfs", 2015.

[5] Embraer S.A, „Embraer," 2017. [Online]. Available: http://www.embraer.com.

[6] AIRBUS, „AIRBUS S.A.S.," 2017. [Online]. Available: http://www.airbus.com/support-services/airport-operations/aircraft-characteristics/.

[7] H. Assler, „Design of Aircraft Structures under Special Consideration of NDT," in *9th European Conference on NDT*, Berlin, Germany, 2006.

[8] I. K. Jennions, Integrated Vehicle Health Management - Perspectives on an Emerging Field, Warrendale: SAE International, 2011.

[9] C. R. Farrar und K. Worden, Structural health monitoring : a machine learning perspective, John Wiley & Sons, Ltd, 2013.

[10] I. K. Jennions, Integrated Vehicle Health Management: The Technology, SAE International, 2013.

[11] LORD Corporation, „LORD, MicroStrain Sensing Systems," 2016. [Online]. Available: http://www.microstrain.com/.

[12] M. Ekman, „KTH," [Online]. Available: https://www.kth.se/polopoly_fs/1.146328!/Menu/general/column-content/attachment/3_Ekman_Saab.pdf.

[13] K. J. Keller, J. Maggiore, R. Safa-Bakhsh, W. Rhoden und M. Walz, Sensory Prognostics and Management System (SPMS), SAE International, 2012.

[14] F. Thielecke, Lecture "Flugzeugsysteme", 2015.

[15] I. Moir, A. Seabridge und M. Jukes, Civil Avionics Systems Second Edition, John Wiley & Sons, Ltd, 2013.

[16] FAA, Aviation Maintenance Technician Handbook–Airframe - Volume 1, Aviation Supplies and Academics, Inc., 2012.

[17] M. S. B. Mahmoud, C. Guerber, N. Larrieu, A. Pirovano und J. Radzik, Aeronautical Air−Ground Data Link Communications, ISTE Ltd, 2014.

[18] C. Spitzer, U. Ferrell und T. Ferrell, Digital Avionics Handbook, Third Edition, CRC Press, 2014.

[19] F. A. Lucchesi und C. T. Wolff.USA Patent US 8220038 B1, 2008.

[20] S. Sun, „ACARS Data Identification and Application in Aircraft Maintenance," in *First International Workshop on Database Technology and Applications*, Wuhan, Hubei, 2009.

[21] J. Walton, „Inflight connectivity shows MRO benefits: Lufthansa Technik," 03 September 2015. [Online]. Available: https://www.runwaygirlnetwork.com/2015/09/03/inflight-connectivity-shows-mro-benefits-lufthansa-technik/.

[22] Q. A. Acton, Advances in Information Technology Research and Application: 2013 Edition, Atlanta, Georgia: ScholarlyEditions, 2013.

[23] C. Grothe, Updates für Onboard-Datenbanken, Technische Universität Darmstadt, 2005.

[24] J. N. Tavares, Data communications between an airplane Airbus A350 and the ground infrastructure, Lisbon, Portugal, 2014.

[25] J. Dollmayer und U. Carl, Einfluss des Leistungsbedarfs von Flugzeugsystemen auf den Kraftstoffverbrauch, Hamburg: Technische Universität Hamburg-Harburg, Arbeitsbereich Flugzeug-Systemtechnik, DLRK 2004, DGLR-JT2004-261, 2004.

[26] N. Meier, „Jet Engine Specification Database," 5 April 2005. [Online]. Available: http://www.jet-engine.net/civtfspec.html.

[27] International Air Transport Association (IATA), „Fuel Price Analysis," 2017. [Online]. Available: http://www.iata.org/publications/economics/fuel-monitor/Pages/price-analysis.aspx.

[28] H. Meyer, Literature based screening of Integrated Vehicle Health Management in European Aircraft, Hamburg: Air Transportation Systems of Hamburg University of Technology, 2015.